Arab J Geosci (2017) 10: 298
DOI 10.1007/s12517-017-3075-0

ORIGINAL PAPER

Separation, upgrading, and mineralogy of placer magnetite in the black sands, northern coast of Egypt

Abdel-Aal M. Abdel-Karim[1] · **Mohamed G. Barakat**[2]

Received: 25 January 2017 / Accepted: 22 June 2017 / Published online: 10 July 2017

Abstract The black sand magnetite is a raw material to produce iron and steel. High content magnetite in the top meter beach sands of the north-west of El-Burullus Lake of Egypt is separated and mineralogically and geochemically investigated. Magnetite content obtained by laboratory techniques varies between 2.92 and 0.11 wt%, with 1.15 wt% average. It represents about one third of the total economic heavy mineral (31.6 wt%). The western and northern halves of the study area are richer in magnetite content (1.33–1.51 wt%) than the eastern and southern halves (0.80–0.98 wt%). On the other hand, the average value of magnetite obtained by ore dressing techniques is 1.13 wt% with a recovery of 98.3 wt%. About 306 samples at a 1-m depth of a grid pattern 200 m × 200 m nearly parallel and perpendicular to the shoreline were covered the area. Microscopic study shows that the magnetite concentrate occurs as irregular, octahedral, or abnormal spherical grains and represented either by fresh homogeneous black or heterogeneous exsolved grains with ilmenite. XRD data indicate that the sample is composed mainly of magnetite grains. Grain size distribution suggests a very fine sand size modal class of more than 93 wt% of the particles. The fine sand size class contains 5.21 wt% magnetite grains. The abnormal spherical grains are mostly more coarser than the associated magnetite concentrate, so they are easily concentrated by sieving process. The contents of iron oxide and titanium dioxide of octahedral magnetite vary from 73.3 to 91.5 and 2.0 to 16.0 wt%, with 85 and 6.0 wt% averages, respectively. On the other hand, these contents of the abnormal spherical one are variable from 81.4 to 95.6 wt%, with 90.3 wt% averages for iron oxide and from 0.3 to 4.0 wt%, with 1.3 wt% average for titanium dioxide. The tonnage of magnetite using laboratory and ore dressing techniques is 182,850 and 179,670 t, respectively. The chemical data of the investigated magnetite suggest their basic volcanic rock origin of the Blue Nile provenance and can be considered as a good indicator for the volcanic source of the Ethiopian plateau.

Keywords Separation · Mineralogy · Chemistry · Magnetite · Black sands · Northern Egypt

✉ Abdel-Aal M. Abdel-Karim
am_abdelkarim@hotmail.com

[1] Geology Department, Faculty of Science, Zagazig University, Zagazig 44519, Egypt

[2] Nuclear Materials Authority, 530-Maadi, Cairo, Egypt

Introduction

The Egyptian black sand extends along the beaches of the northern parts of the Nile Delta especially at Rosetta and Damietta. The Egyptian beach magnetite occurs as a relatively high content in naturally highly concentrated surfaced black sand at definite beach zones characteristic by severe erosion. It is considered as the second economic abundant mineral of the seven essential more abundant minerals: ilmenite, leucoxene, garnet, zircon, rutile, and monazite from the black sands deposited at Rosetta and Damietta (Fig. 1). The mineralogy and chemistry of six economic heavy minerals along the northern coast of Egypt were recently studied by Abdel-Karim et al. (2016).

Magnetite is often mined as a raw material to produce iron and steel on which the modern societies are based. Hammoud (1966) concluded that the black sand magnetite has low grade in iron and steel production due to their impurity contents especially chromium and vanadium. On the other hand, Nofal et al. (1980) studied the beneficiation of the black sand titanomagnetite and proved its suitability for iron and steel

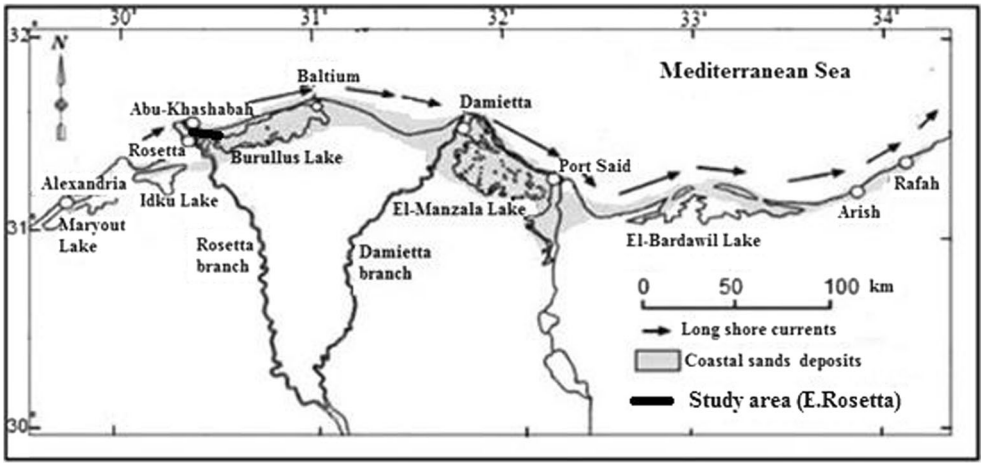

Fig. 1 Map showing location of the study area and distribution of the black sand deposits in the northern coastal zone of Egypt

industry. Magnetite is a ferromagnetic mineral with chemical composition ferrous-ferric oxide (Fe^{2+}, Fe_2^{3+} O_4). It is a combination of wustite (FeO, 31.03 wt%) and hematite (Fe_2O_3, 68.97 wt%). Deviation from theoretical proportion, it commonly takes place during both magmatic differentiation and weathering cycle. Replacement occurring in magnetite includes the partial substitution of Al, Cr, and V for Fe^{3+} whereas Fe^{2+} may be partially replaced by Ni, Co, Zn, Mg, Mn, and Ca (Deer et al. 1975).

Hammoud (1966) suggested that the Egyptian black sand magnetite shows evidence of oxidation with low Fe^{2+}/Fe^{3+} ratio, lower magnetic susceptibility, and low specific gravity (4.76 g/cm^3). The lower specific gravity of the Egyptian magnetite concentrate attributed to unliberated light minerals such as quartz, feldspars, and pyroxene minerals adhered to magnetite grains.

Due to heterogeneous sources of the Egyptian black sand magnetite, it contains considerable amounts of titanomagnetite in addition to small amounts of manganese-, vanadium-, and chromium-rich varieties. The titanium-free magnetite forms only about 15 wt% of the total Egyptian magnetite (Wassef and Mikhail 1981). Abdel-Karim et al. (2016) proved that the spherical magnetite grains are higher in Fe_2O_3 than those of euhedral-shaped grains. According to El-Kammar et al. (2011), the opaque Fe-Ti minerals such as ilmenite and magnetite are considered as good indicators of the volcanic source of the Ethiopian plateau.

The Egyptian black sand magnetite grains exhibit dull black to brownish black color; the brownish tint can be attributed to their alteration and/or oxidation process, in addition to the probable presence of magnetite–ilmenite intergrowths. Different types of magnetite–ilmenite intergrowths and their origin were studied previously by many workers such as Boctor (1966), Basta (1972), Dewedar (1997), and El-Nahas (2002). Due to there is no detailed previous work, the authors believe that this paper presents, for the first time, separation and mineralogy of placer magnetite of Egypt.

Recently, magnetite mixed with green silicate minerals is required for making fertilizers and land reclamation. As a result of the growing demand for the ore, this contribution

Fig. 2 Satellite photo showing the zones of erosion and accretion along the shoreline north of the study area

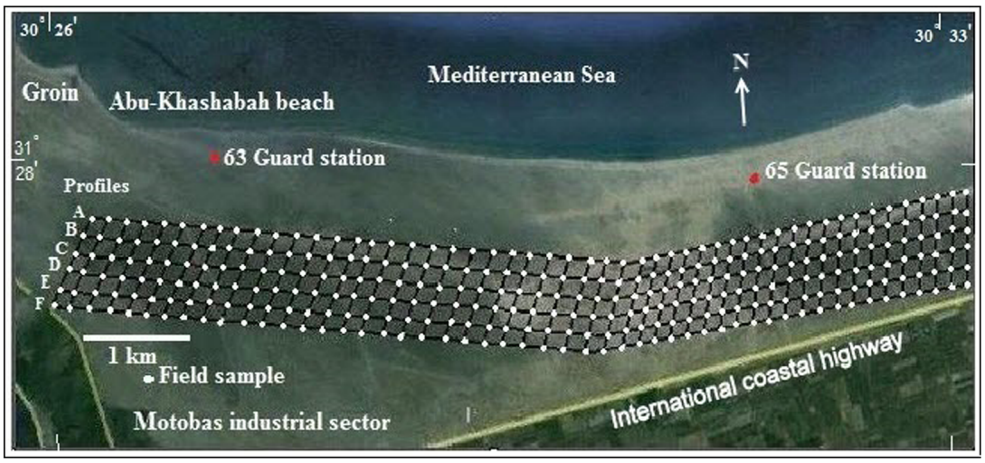

Fig. 3 Satellite map showing location of field samples

aims to separation and mineralogy of magnetite of the top meter sands north-west of El-Burullus Lake, Egypt, using laboratory and ore dressing techniques. The objective of this study is to improve the available data based on the composition, upgrading, origin, and reserve of this potential magnetite.

The study area

The study area lies on the Mediterranean Sea coast, about 8 km east of Rosetta distributor mouth, north-west of El-Burullus Lake (Fig. 1) between longitudes 30° 25′ 48″ and 30° 33′ 00″ E and latitudes 31° 26′ 42″ and 31° 27′ 18″ N. The coastal plain of the study area is nearly rectangular in shape, 10 km long parallel to the shoreline and 1-km width nearly perpendicular to the shoreline. El-Sahel (coastal) drain which runs parallel to the shoreline divided the east Rosetta coastal plain area into northern and southern sectors. The northern sector is bounded from the north by the Mediterranean Sea and from the south by El-Sahel drain. It is characterized by relatively highly concentrated black sand especially in the near shore area. But this sector is affected greatly by marine erosion and continuous retreat of the shoreline. The southern sector (study area) is bounded from the north by El-Sahel drain and from the south by the international highway and is characterized by a light tone and rich in clay and organic matter. This sector is far from marine erosion and free from human activities (Fig. 2).

Table 1 Average values of fine percentage in each kilometer of the study area

Kilometer number		Fines (wt%)
West	First	21.04
	Second	16.25
	Third	19.34
	Fourth	16.85
	Fifth	19.03
	Sixth	13.68
	Seventh	12.92
	Eighth	19.25
	Ninth	21.14
East	Tenth	19.93

Sampling and methodology

The coastal plain sector of the study area was covered by 306 samples to a depth of 1 m at the intersection of a grid pattern 200 m × 200 m nearly parallel and perpendicular to the shoreline (Fig. 3). The collected samples distribute along six profiles parallel to the shoreline. These profiles had given the symbols, A, B, C, D, E, and F from north to south, respectively. Every profile comprises 51 samples taken the symbol of the profile and numbered from 1 to 51 from west to east. The northern profile (A) runs with El-Sahel coastal drain. The distance between the southern profile (F) and the international coastal road ranges from 2000 m in the west to 200 m in the east.

During exploitation of the black sand deposits, the presence and distribution of fines (sizes finer than the coarse silt) are an important parameter, where these materials cause many problems during mining processes of the beach placers. Therefore, the mining plan must take such problem in consideration. Also, the high clay content in the field sediments causes some problems during concentration and separation of economic heavy minerals using ore dressing techniques especially shaking table.

The collected field samples are composed of wet loose sediments. Firstly, each field sample was subjected to sun drying and disaggregation process. Each dry field sample (weighing about 11 kg) was split into two halves using John's splitter. One of them was kept in a bag as a reference sample, and the second was subjected to splitting again to

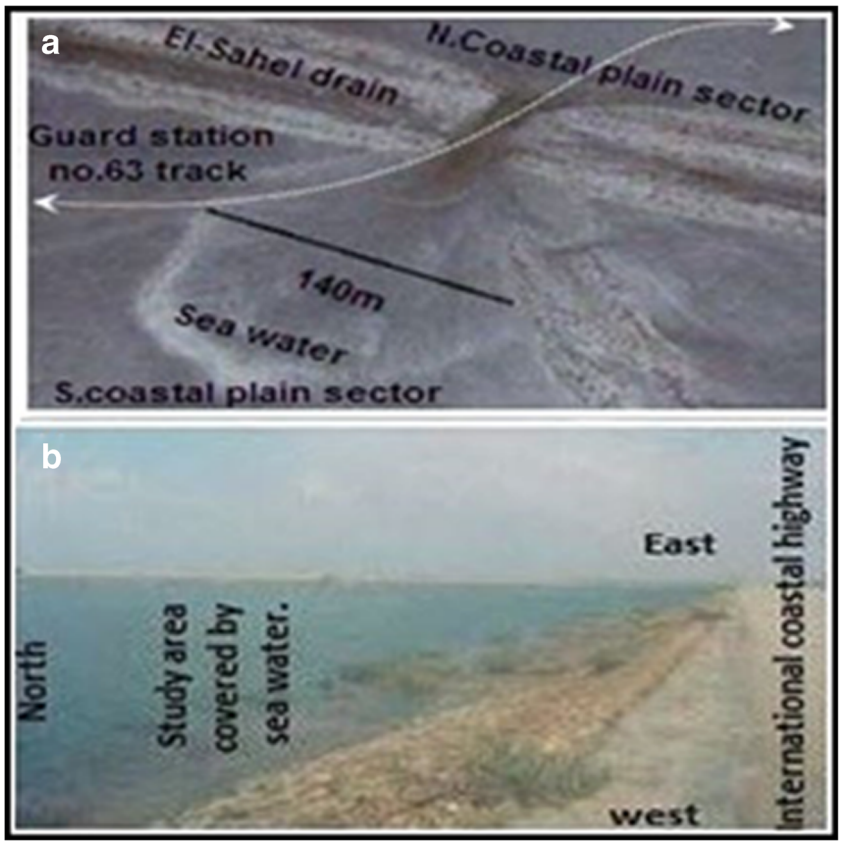

Fig. 4 **a** Satellite photo showing the distribution of El-Sahel drain and the coastal plain sectors and **b** field photograph showing southern coastal flat stretch covered by sea water during winter season

obtain a representative sample weighing about 200 g for the different analyses while the rest returned to the stored sample.

Each representative sample was weighed and put in a 2-L-size beaker filled with tap water and using an electric stirrer for about 5 min to liberate the different minerals particles composing the sample. Then, the sample was left to rest for a time suitable to settle all sizes larger than fine silt size. The upper two thirds of the water depth with its suspended materials was decanted using a siphon to avoid the escape of any sand particle during decantation. The process was repeated several times till the decanted water becomes clear.

The organic matter content in each washed sample was leached by adding hot hydrogen peroxide (3%) to the sample and stirred for about 10 min and left at rest. Then, the sample was periodically stirred with a glass rod till the effervescence stopped indicating complete leaching of the organic materials. The leached organic matters were removed from the sample by stirring in water and decantation for several times. The distilled water was used in the last wash to remove any salt remains.

The clean samples were then dried and weighed. The average values of fine percentage in each kilometer were calculated, and the results are shown in Table 1. The fines vary from 0.72 to 74.08 wt% with 18.00 wt% average. The ninth and first kilometers respectively contain the highest fine percentage compared with the other kilometers. The highest fine percentage (21.14 wt%) was located at the ninth kilometer sediment whereas the lowest value (12.92 wt%) was located at the seventh kilometer which is characterized by the distribution of sand hillocks.

It was noticed that in winter season and during stormy condition, the coastal plain of the study area was covered by sea water rich in fines which are derived from the clay lenses of the continental shelf by erosion process (Fig. 4). So, the high content of fines in the study area may be attributed to the above phenomenon. Also, it was noticed that the western and eastern sectors of the study area are characterized by the distribution of marshes and low land areas rich in clay content.

Concentration and separation

Heavy liquid separation

Representative samples each of which weighing about 40 g from the 306 previously prepared samples were subjected to heavy mineral separation using Bromoform (2.8 g/cm^3) and Clerici's solutions (3.7 g/cm^3). The obtained heavy fractions from the Bromoform separation were subjected to Clerici's solution separation in order to separate the heavy economic minerals in the sink layer or heavy fractions and the colored silicates in the float fractions. The average percentages of

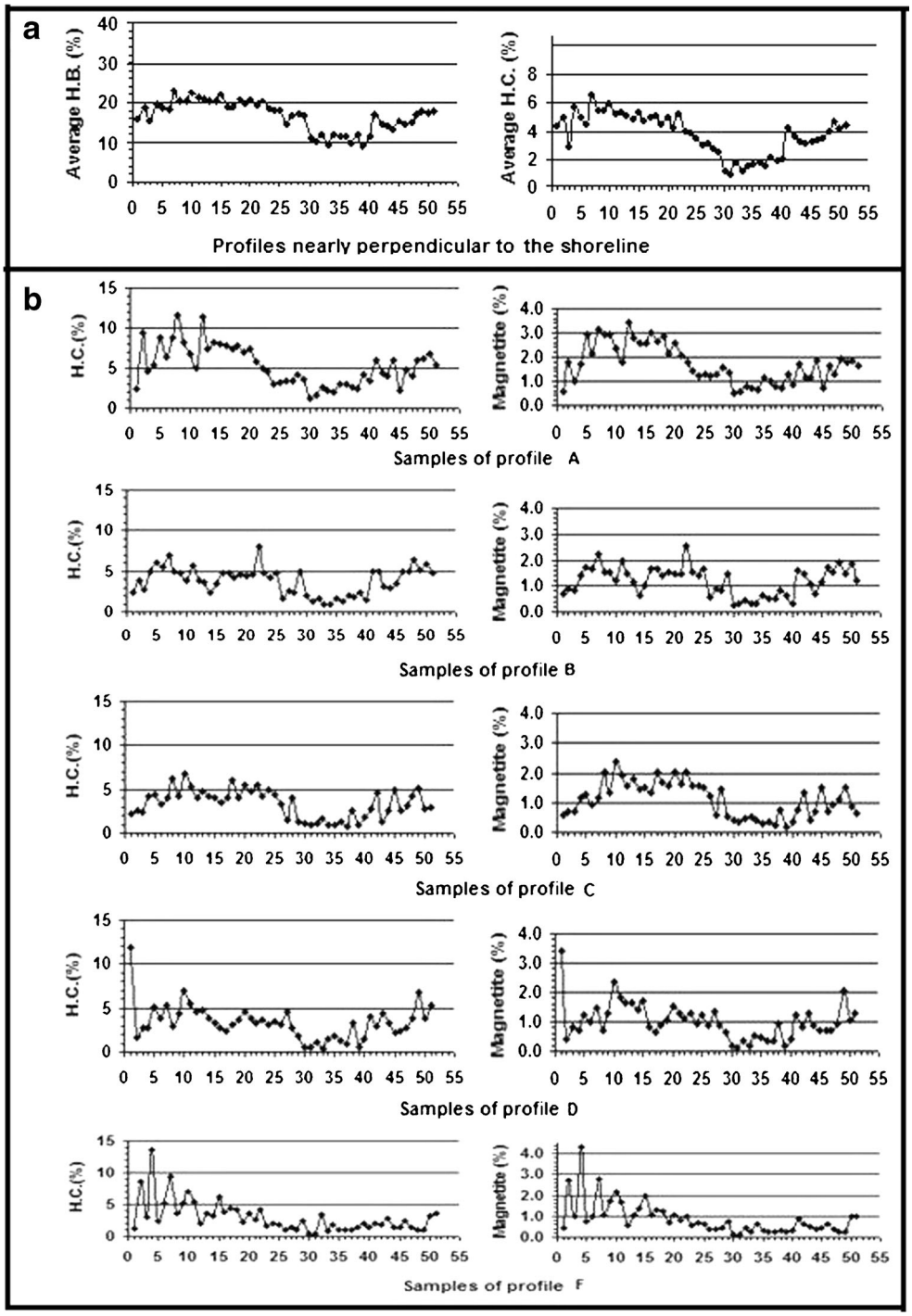

Fig. 5 Graphic representation showing **a** average percentages of Bromoform and Clerici's solution heavy fractions along 51 profiles and **b** economic heavy mineral percentage (H.C. wt%) and magnetite wt% along six profiles parallel to the shoreline

Bromoform (H.B. wt%) and Clerici's solution (H.C. wt%) heavy fractions along 51 profiles nearly perpendicular to the shoreline are graphically represented in Fig. 5a. The Bromoform heavy fractions (total heavy minerals) which are represented mainly by economic minerals and green silicate minerals vary from 34.22 to 4.78 wt% with an average value of 16.60 wt% whereas the Clerici's solution heavy fractions which are represented mainly by economic heavy minerals vary from 13.58 to 0.38 wt% with an average value of 3.70 wt%. Figure 5b exhibits three zones along the shoreline: the western zone (about 4 km long) has relatively highly concentrated sediments, the eastern zone (about 3 km long) has intermediate concentration of economic heavy minerals, and the middle one (about 3 km long) has low concentrated sediments. During field works, it was noticed that the middle zone is characterized by the distribution of abandoned old fish

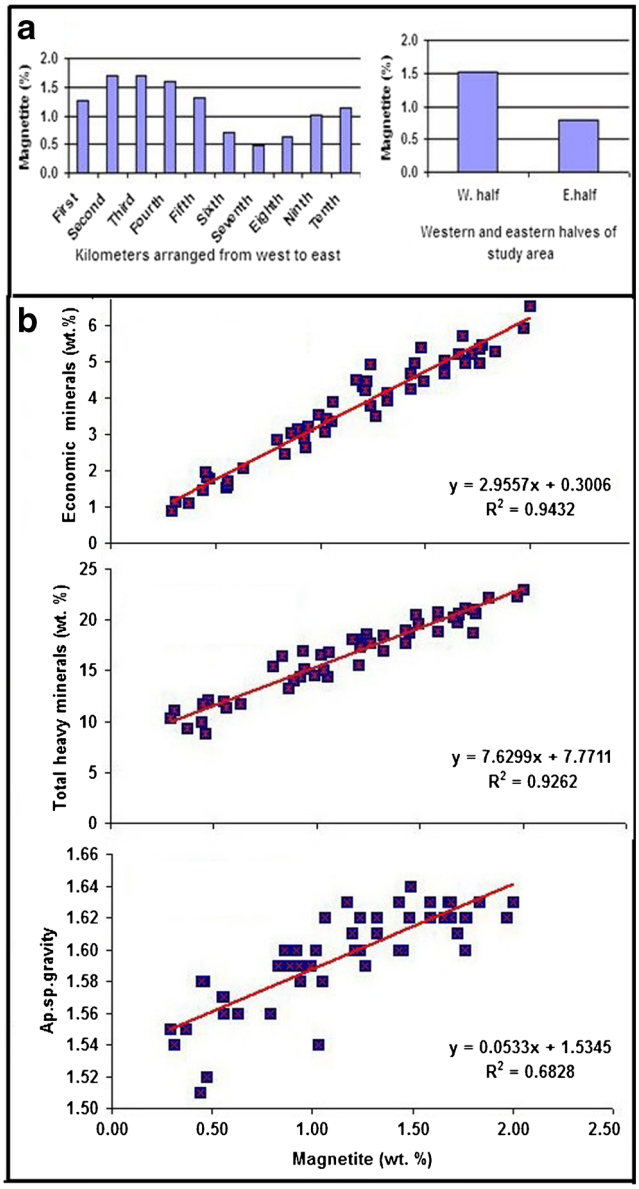

Fig. 6 **a** Graphic representation showing the average percentages of magnetite along 10 km^2 as well as the western and eastern halves of the study area and **b** scatter plot diagrams show the relationship between the average values of magnetite and the economic heavy minerals, total heavy minerals, and average of apparent specific gravity

farms, which is prepared by scraping the relatively highly concentrated top meter sands.

Magnetic separation

The magnetite content in the different heavy parts was separated using a Frantz FerroFilter magnetic separator (permanent magnet). The separated magnetite was weighed, and its percentage relative to the weight of the original sample was calculated and is plotted in Fig. 6a.

The magnetite content varies between 0.11 and 2.92 wt% with an average value of 1.15 wt%. It represents about one third of the total economic minerals, and there are close relations between the concentration of magnetite and the concentration of the other economic heavy minerals (H.C. wt%) along the different profiles. So, the magnetite content, which can be easily obtained by using of a hand magnet, can be threw the light on the concentration of the associated economic minerals.

Table 2 The average percentages of magnetite (wt%) along 10 km arranged parallel to the shoreline

Kilometers		Magnetite (wt%)			
West	First	1.26	1.56	W. half 1.51	1.15
	Second	1.69			
	Third	1.70			
	Fourth	1.59			
	Fifth	1.31	0.83		
	Sixth	0.72		E. half 0.80	
	Seventh	0.47			
	Eighth	0.64	0.93		
	Ninth	1.01			
East	Tenth	1.15			

The average percentages of magnetite along 10 km arranged from west to east parallel to the shoreline as well as the western and eastern halves of the study area are listed in Table 2 and shown in Fig. 6a. The magnetite content of the study can be divided into three zones parallel to the shoreline, the western zone (4 km^2) has relatively highly concentrated sands (1.56 wt%), the eastern zone (3 km^2) has moderately concentrated sands (0.93 wt%), while the middle zone (3 km^2) has low concentrated sands (0.83 wt%). The magnetite percentage in the western and eastern halves of the study area is 1.51 and 0.80 wt%, respectively.

Because magnetite is a ferromagnetic mineral, its percentage can be easily obtained by the using of a hand magnet. So, the average values of magnetite content, the apparent specific gravity, the total heavy minerals, and the economic heavy minerals along 51 profiles nearly perpendicular to the shoreline were graphically represented in scatter plot diagrams (Fig. 6b). The obtained results show good positive correlations between the average contents of magnetite and the other mentioned variables.

Ore dressing concentration

Frankly speaking, the concentration and separation of magnetite and other economic heavy minerals using ore dressing techniques are the closest to reality, cheapest, fastest, and least dangerous to human health compared with the laboratory (heavy liquid) techniques. These techniques are very important in concentration and separation of economic heavy minerals on industrial scale using a suitable flowsheet based on

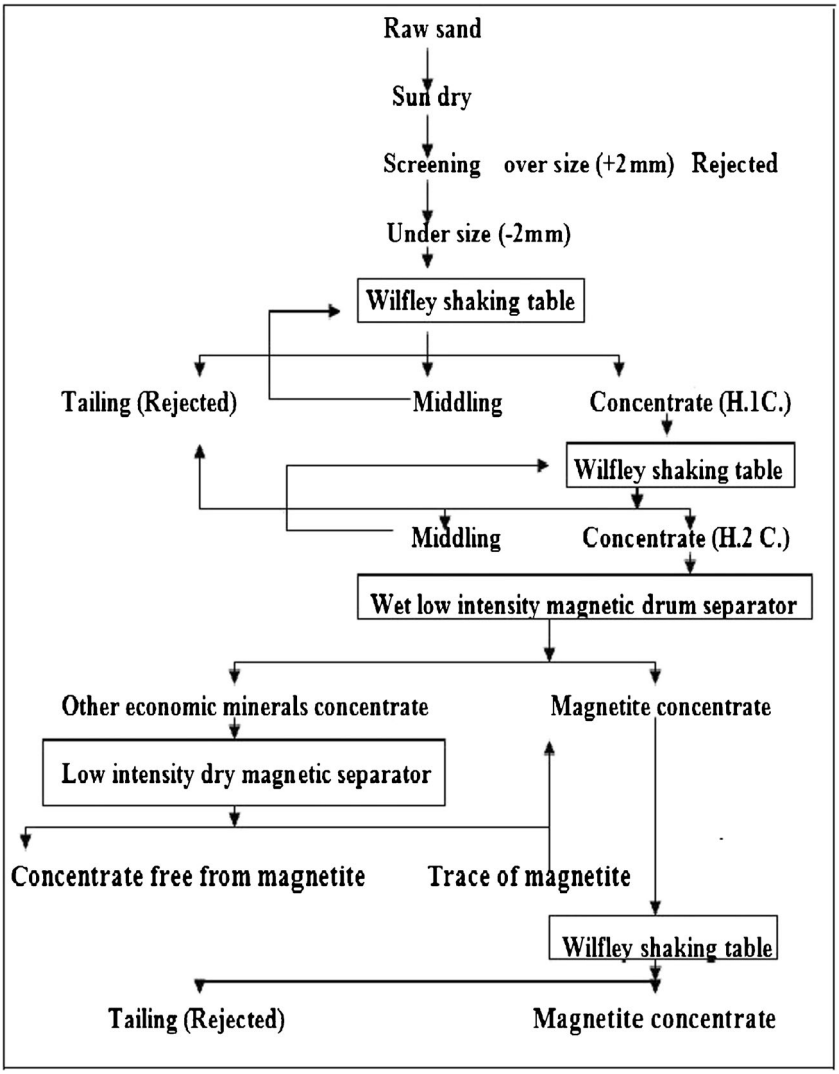

Fig. 7 The different steps of the flowsheet used for concentration and separation of magnetite

the physical and chemical characteristics of mineral grains. The representative samples were prepared from the collected field samples. Each sample weighing about 6.5 kg was subjected to heavy mineral concentration and separation of magnetite using a simple flowsheet including gravitational and magnetic methods (Fig. 7). Each prepared sample was subjected firstly to sun drying and screened using a 2-mm screen to remove coarse waste and shell fragments.

Gravity concentration process is the oldest beneficiation method known to mankind. It is an environment-friendly process, which utilizes simple equipment with few moving parts. Throughout the history of mineral processing, many different

Table 3 Comparison between machine and feed variables

Machine variables	Feed variables
- Stroke:	- Solid characteristics:
Length and frequency	Specific gravity, shape, and size range of the particles.
- Inclination:	- Feed rate.
Side and longitudinal slope.	- Pulp characteristics:
- Riffles pattern.	Flow rate.
- Roughness of the deck surface.	Density.
- Splitter position.	Wash water.

Fig. 8 Separation of economic heavy minerals using half-size Wilfley shaking table

types of gravity separation devices have been utilized (e.g., Reichert cone, Humphrey spiral, and Wilfley shaking table). Each of these devices takes advantage of density differences between valuable and gangue minerals. Besides the specific gravity of mineral grains, other factors such as the size and shape of the particles affect the relative movement and hence the separation process. The ease or difficulty of separation depends upon the relative differences in these factors. The half-size shaking table was selected as an appropriate method for the concentration and separation of economic heavy minerals. This is because the field sample weight is suitable for the feed rate of the shaking table (km), but not suitable for Reichert cone or Humphrey spiral (t). Also, shaking tables are less expensive than other concentration hardware such as Reichert cone and spiral concentrators. This is the primary reason why most small-to-medium operations usually start with a table until they start making some money to expand their operations with other types of concentration equipment. The effective separation of mineral particles using the shaking table requires a suitable adjustment of the operation condition

Table 4 The operation condition for the wet tabling of the field samples

Parameters	Condition
Feeding rate (kg/h)	100
Feed pulp density (%)	10
Washing cross-flow water (L/min)	70
Deck side tilt (mm/m)	12
Deck longitudinal tilt (mm/m)	5.7
Stroke length (mm)	10
Stroke frequency (rpm)	310

variables. According to Burt (1989), Barakat (2004), and Moustafa (2007), these variables can be classified into machine variables and feed variables (Table 3).

The Wilfley shaking table may be used for rough concentration or for cleaning process. In general, the cleaning operation was optimized by using less feed, less water, less tilt as much as possible, and shorter length of stroke beside a low speed of the deck. On contrary, the rough concentration required more feed, more water, more tilt, and longer stroke. Using half-size Wilfley shaking table (Fig. 8), a circuit of two tabling stages is carried out under the condition shown in Table 4. The table deck side tilt is 12 mm/m, deck longitudinal tilt is 5.7 mm/m, and stroke frequency is 310 rpm. The table feed rate is 90 kg/h, and the washing cross flow water 70 L/min.

In the first stage, the beach sands were divided into three fractions, concentrate (H1.C), middling, and tail fractions. Most of gangue minerals which consist mainly of quartz and green silicate minerals are removed and rejected in the obtained first tailing fraction. A considerable amount of green silicate minerals in association with some of economic minerals is separated in a middling fraction from the first tabling stage. The middling fraction of the first stage was retreated again to minimize loss of the economic minerals in the tail fraction. The obtained heavy mineral concentrate (H1.C) was treated again as in the first stage to obtain final economic heavy mineral concentrate (H2.C) of a minimum content as possible of gangues and a minimum loss of economic minerals in the tails. The average percentages of H1.C and H2.C are listed in Table 5 and plotted in Fig. 9a. This figure shows close relations between the distributions of total and economic heavy minerals. Therefore, based on the distribution of total and economic heavy minerals, the study area can be divided into three zones: the western, the eastern, and the middle zones. The highly concentrated top meter sands of the middle zone were scraped during the preparation of fish farms in this area.

Each economic heavy mineral concentrate of the Wilfley shaking table was subjected to magnetite separation. The separation was carried out by low-intensity wet drum magnetic separator for big and highly concentrated samples or by the using of a Frantz FerroFilter magnetic separator for small and diluted samples. The separated magnetite was weighed; its percentage relative to the weight of the original sample was calculated (Table 6) and plotted in Fig. 9b. A close relation between the distribution of magnetite and the distribution of total and economic heavy minerals is observed.

The economic mineral concentrates (free from magnetite) are mixed together to form one representative sample. This sample is subjected to magnetic fractionation using low-intensity reading cross-belt magnetic separator. The operating variables of cross-belt magnetic separator include the following:

Table 5 Average percentage of total heavy mineral (H1.C) and the economic heavy mineral (H2.C) along 51 profiles nearly perpendicular to the shoreline separated by ore dressing technique

Profile	Shaking table conc.		Profile	Shaking table conc.		Profile	Shaking table conc.		Profile	Shaking table conc.	
	H1.C (wt%)	H2.C (wt%)		H1.C. (wt%)	H2.C (wt%)		H1.C. (wt%)	H2.C (wt%)		H1.C. (wt%)	H2.C (wt%)
1	7.47	4.86	14	7.29	5.25	27	5.03	2.55	40	3.49	2.16
2	7.72	5.06	15	8.67	5.62	28	4.23	2.67	41	5.51	4.46
3	5.08	3.16	16	6.07	4.51	29	4.15	2.85	42	4.57	3.47
4	9.09	6.39	17	6.77	4.66	30	2.35	1.15	43	4.91	3.45
5	7.48	4.91	18	6.54	4.48	31	2.33	0.97	44	4.58	3.68
6	6.97	4.72	19	7.08	4.62	32	3.51	1.98	45	5.16	3.61
7	8.67	6.28	20	7.07	4.94	33	2.56	1.36	46	5.64	3.68
8	8.34	6.27	21	6.44	4.44	34	3.02	1.64	47	4.76	3.01
9	8.56	5.96	22	6.36	4.64	35	3.42	1.64	48	5.77	3.96
10	8.52	5.93	23	5.87	4.05	36	3.85	1.89	49	6.22	4.54
11	8.12	5.48	24	5.3	3.55	37	2.67	1.47	50	6.48	4.38
12	8.21	5.26	25	5.68	3.62	38	3.71	2.15	51	6.87	4.76
13	7.75	5.23	26	4.34	2.64	39	3.57	2.02	Av.	5.76	3.84

1. Field strength (measured indirectly and controlled by ampere adjustment of the electromagnet): field strength is typically up to 19,000 gauss. The magnetic field strength can be varied from minimum of 9500 gauss (0.90-cm air gap) on the first cross belt to 19,000 gauss (0.40-cm air gap) on the last one.
2. Pole air gap (distance between the upper poles and the feed belt): a pole air gap ranges from 9 to 4 mm.
3. Feed rate (about 1 t/h): the actual feed rate capacity depends on its nature and the performance required.
4. Chute splitter position: a splitter is provided in each cross-belt product collection box to enable a middling as well as a magnetic concentrate to be produced.
5. Thickness of cross belt: the thickness of cross belt should be thin as possible, usually about 1 mm thick.
6. Speed of feed belt: the speed of feed belt is affected on the capacity and recovery of separation. The usual speed of the feed belt is 4 rpm.
7. Speed of takeoff belt (cross belt): the speed of takeoff belt (cross belt) is affected by the kind of material removed

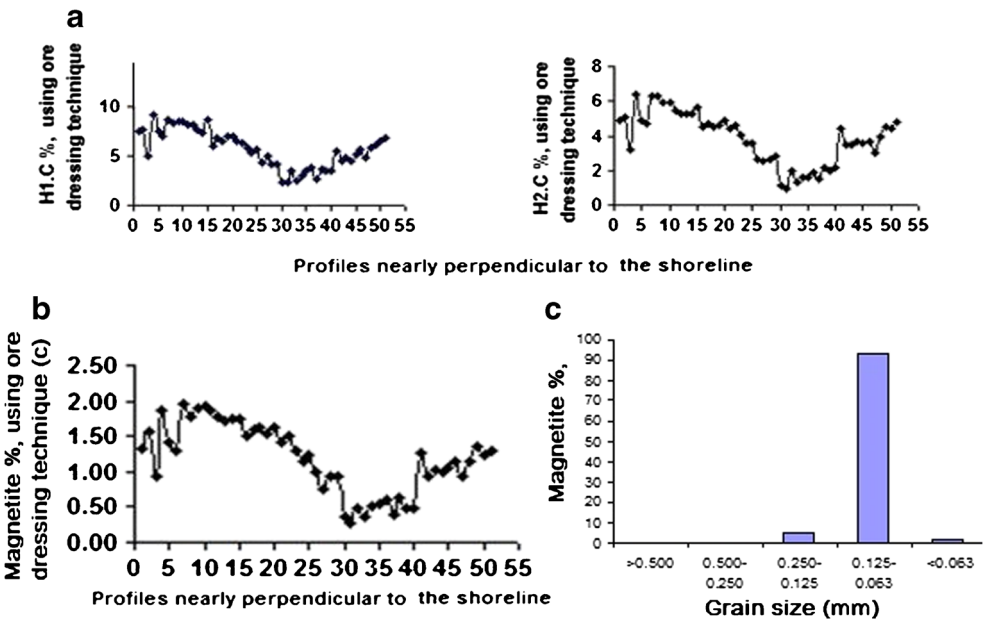

Fig. 9 Graphic representation showing **a** average values of total (H1.C) and economic (H2.C) heavy mineral percentages obtained by ore dressing techniques along 51 profiles, **b** magnetite percentage along 51 profiles separated by ore dressing technique, and **c** frequency showing the grain size distribution of magnetite

Table 6 Average magnetite percentages along 51 profiles nearly perpendicular to the shoreline separated by the using of ore dressing technique

Profile	Magnetite (wt%)	Profile	Magnetite (wt%)	Profile	Magnetite wt%	Profile	Magnetite (wt%)
1	1.33	14	1.75	27	0.74	40	0.48
2	1.57	15	1.76	28	0.92	41	1.28
3	0.93	16	1.51	29	0.94	42	0.93
4	1.87	17	1.6	30	0.36	43	1.01
5	1.42	18	1.62	31	0.27	44	0.99
6	1.3	19	1.53	32	0.47	45	1.04
7	1.95	20	1.64	33	0.36	46	1.13
8	1.77	21	1.42	34	0.51	47	0.93
9	1.91	22	1.5	35	0.54	48	1.13
10	1.93	23	1.29	36	0.59	49	1.37
11	1.86	24	1.14	37	0.4	50	1.25
12	1.77	25	1.23	38	0.62	51	1.29
13	1.73	26	0.99	39	0.47	Av.	1.18

and the size of particles. It may be higher with strongly than weakly magnetic materials and higher with fine than coarse particles.

The operating conditions (Table 7) are used to obtain the trace magnetite grains, which may be still present in the economic mineral concentrate. It was noticed that a few green silicate minerals contain magnetite inclusions still present in magnetite concentrate. Therefore, it was subjected to water shaking table to remove the coarse and light green silicate gangues to upgrade the magnetite concentrate. The obtained magnetite content by using of ore dressing techniques attains 1.13 wt% with a recovery of 98.26 wt%.

Results and discussion

Grain size distribution

Grain size distribution of mineral grains is an important factor in concentration and separation of economic heavy minerals using wet gravity and electrostatic and magnetic processes during exploitation of black sands (Lawver et al. 1986; Burt 1989; Kelly and Spottiswood 1989 and Moustafa 1999). Also, the grain size distribution is important in metallurgy and chemical treatments of mineral grains.

The grain size distribution of magnetite of the study area is a unimodal with very fine sand size class, which constitutes more than 93 wt% of the particles. The fine sand size class contains 5.21 wt% from the particles as shown in Table 8 and Fig. 9c. This grain size distribution is consistent with that given by Abdel-Karim et al. (2016) on the heavy minerals in the black sands, along the northern coast of Egypt. The spherical magnetite grains are mostly more coarser in grain size than the associated magnetite concentrate. So, they are concentrated by sieving process and picked using binocular stereomicroscope for studying abnormal shapes and chemistry.

Apparent density of raw sand

Actually, the apparent specific gravity of the Egyptian beach placers is directly proportion to the heavy mineral content as well as the grain size of the deposit (Dabbour 1991). So, the apparent specific gravity is considered as a very simple tool throwing the light on the concentration of heavy economic minerals in the raw sand. Also, the apparent specific gravity of raw sand is necessary for

Table 7 The operating conditions of the reading cross-belt magnetic separator

Condition	First pair magnet			Second pair magnet		Third pair magnet	
	Scalper pole 1	Pole 2	Pole 3	Pole 4	Pole 5	Pole 6	Pole 7
Air gab (mm.)	18	8	6	5	5	4	4
Ampere (A)	5			8		10	
Feed rate (t/h)	0.5						
Speed of feed belt pulley	4 rpm						

Table 8 Grain size distribution of magnetite in the study area

Size fraction (mm)	Magnetite (wt%)
>0.500	0
0.500–0.250	0.08
0.250–0.125	5.21
0.125–0.063	93.04
<0.063	1.67

the transformation of the cubic meters of raw sand to tons during determination of the reserve of economic minerals in tons. Therefore, the apparent specific gravity for each field sample collected from the study area was measured. Each field sample was dried carefully, and a representative sample (1–2 kg) was taken by the using of John's splitter. Each representative sample was weighed and slowly poured inside a calibrated cylinder and compacted very well by shaking to be analogous to the field deposit. The weight of the sand was divided by its volume to obtain the apparent specific gravity. The apparent specific gravity varies from 1.29 to 1.74 g/cm^3 with average value 1.59 g/cm^3. Minimum, maximum, and average values of apparent specific gravity along six profiles parallel to the shoreline in the study area were calculated (Table 9). The average values of apparent specific gravity along 10 km^2 and three zones arranged from west to east of the study area were estimated and are represented in Fig. 10. The apparent specific gravity of the western, eastern, and middle zones is 1.62, 1.59, and 1.58 g/cm^3, respectively.

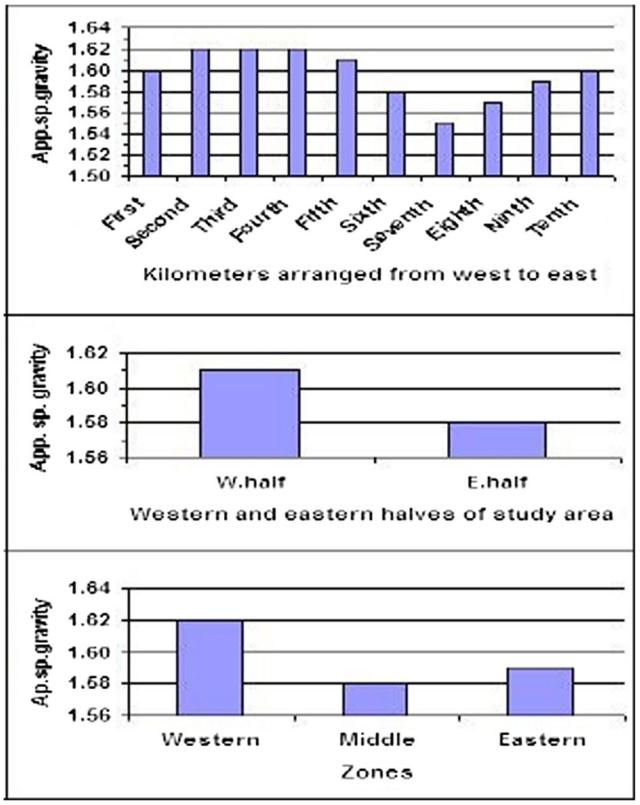

Fig. 10 Histograms showing the average values of apparent specific gravity along 10 km^2 and the western and eastern halves as well as three zones of the study area

Table 9 Apparent specific gravity along six profiles, 10 km^2, zones and halves of the study area

	Profiles					
	A	B	C	D	E	F
Value						
Minimum	1.55	1.48	1.40	1.29	1.41	1.48
Maximum	1.70	1.70	1.64	1.74	1.73	1.69
Average	1.63	1.60	1.59	1.59	1.60	1.58
Kilometer	Zone	Half	Apparent specific gravity			
First	Western	Western	1.60	1.62	1.61	Average
Second			1.62			1.59
Third			1.62			
Fourth			1.62			
Fifth	Middle		1.61	1.58		
Sixth		Eastern	1.58		1.58	
Seventh			1.55			
Eighth	Eastern		1.57	1.59		
Ninth			1.59			
Tenth			1.60			

X-ray diffraction

An X-ray diffraction analysis of abnormal spherical magnetite grains was carried out at the NMA laboratories using a PHILLIPS PW 3710/31 diffractometer attached with the automatic sample changer PW 1775/21, Cu-target tube, and Ni-filter at 40 kV and 30 mA. The X-ray diffraction data are shown in Table 10, which indicates that the sample is composed mainly of magnetite grains.

Table 10 X-ray diffraction data of abnormal spherical magnetite grains

Sample		Magnetite ASTM card No.(19-629)	
dA	I/I_0	dA	I/I_0
2.96	27	2.967	30
2.53	100	2.532	100
2.09	25	2.09	20
1.71	10	1.715	10
1.61	39	1.616	30
1.48	43	1.485	40

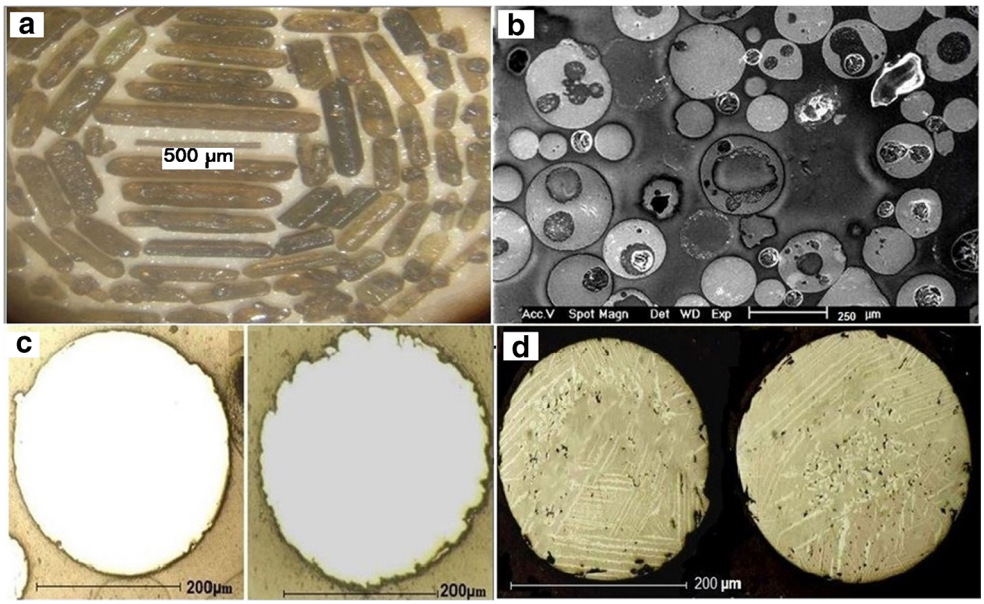

Fig. 11 **a** Stereomicrograph showing long prismatic magnetite grains attached and embedded by fine augite, **b** back-scattered electron image of spherical magnetite polished section showing distribution of air gaps inside spherical grains, **c** photomicrographs of a polished surface showing homogenous magnetite grains, and **d** photomicrographs of a polished surface showing magnetite (*white*)–ilmenite (*gray*) intergrowth grains

Microscopic investigation

Under the binocular microscope, magnetite grains have generally irregular shape where subangular and surrounded particles are recorded beside octahedron crystals. Contact double twins and parting plains are also present. Magnetite concentrate usually obtained by using of a reading cross-belt magnetic separator contains some impurities of green silicate minerals. These minerals are characterized by the distribution of long prismatic magnetite crystals attached by green silicate grains especially augite (Fig. 11a).

Highly magnetic particles of abnormal shapes (spherical, drop and cocoon like, elongated, ovoid, and discoidal) composed mainly of iron oxide were detected. These shapes are formed when the grains moved downward in air. Some spherical grains of different sizes are attached to each other, probably due to collision of these grains together during movement

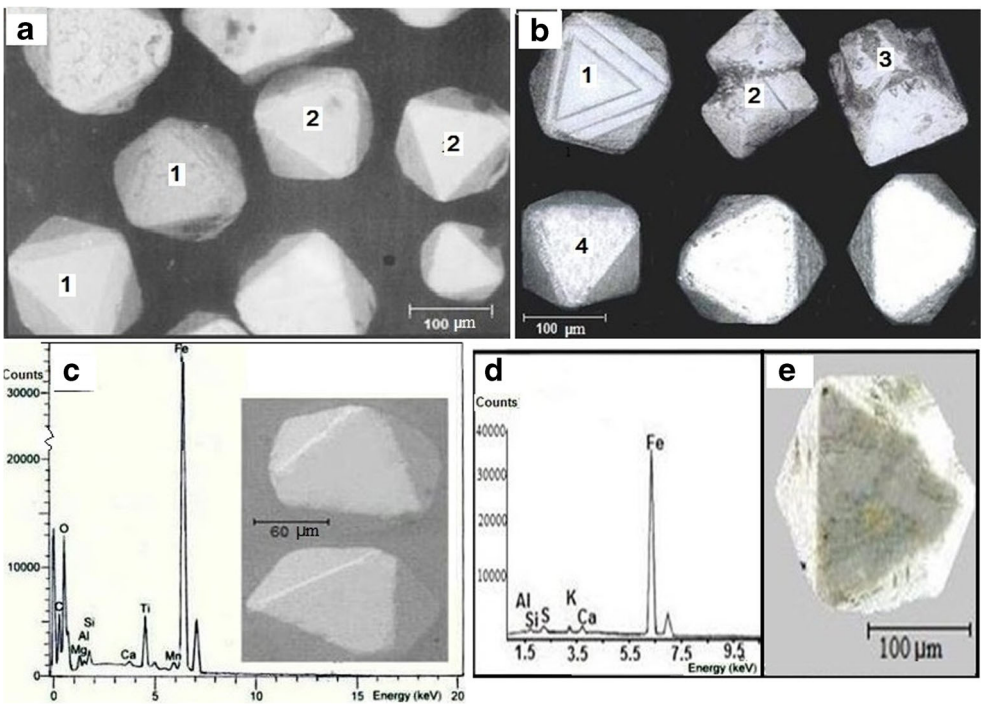

Fig. 12 **a** Back-scattered electron images showing *1* composite crystals, and *2* octahedron; **b** back-scattered electron images showing *1* triangle parting plains, *2* triple twins, *3* double twins, and *4* octahedron; **c** back-scattered electron image and ESEM chemical analysis of octahedral magnetite crystal; **d** ESEM chemical analysis; and **e** stereomicrograph showing an altered octahedral magnetite crystal

Table 11 Chemical analysis of ten magnetite grains

Oxide	G.1	G.2	G.3	G.4	G.5	G.6	G.7	G.8	G.9	G.10
Fe_2O_3	87.60	84.89	84.67	90.84	77.13	90.57	91.53	73.29	78.80	91.10
TiO_2	6.42	5.31	6.01	3.40	12.98	1.95	2.92	16.07	2.45	4.50
MnO_2	0.50	1.78	1.45	0.50	0.30	0.45	0.00	0.00	1.25	0.00
Cr_2O_3	0.59	0.49	0.55	0.24	0.50	0.29	0.20	0.00	0.61	0.20
V_2O_3	0.57	0.52	0.73	0.26	0.99	0.25	0.33	0.00	0.25	0.26
MgO	0.80	0.96	0.75	0.40	1.00	1.60	0.00	2.69	3.19	0.00
CaO	0.30	0.36	0.56	0.29	0.22	0.51	0.38	0.00	1.65	0.66
SiO_2	1.50	3.12	2.29	1.63	5.16	1.93	2.66	3.48	9.54	1.21
Al_2O_3	1.71	2.06	2.99	1.39	1.72	1.95	1.31	4.47	2.26	0.99

in air when they were in semi-molten state. Some grains are massive and contain air gaps of different sizes (Fig. 11b).

Ore microscopy of the studied magnetite suggests that there are two main groups: highly magnetic homogenous grains (Fig. 11c) and relatively weakly magnetic exsolved magnetite–ilmenite intergrowth grains (Fig. 11d).

Scanning electron microscope

Euhedral magnetite crystals

Complete euhedral crystals of magnetite were picked from magnetite concentrate including composite crystal, triple octahedral twin, double octahedral twin, perfect octahedral crystal, and octahedral crystal with perfect parting plains (Fig. 12a, b). They were subjected to chemical analyses using an environmental scanning electron microscope. The energy-dispersive X-ray and the back-scattered electron image are represented in Fig. 12c, d, and the chemical composition of these grains is given in Table 11. The iron oxide (e.g., Fe_2O_3) content ranges from 73.29 to 91.53 wt% with an average value 85.04 wt%. Sometimes, magnetite contains titanium in small amounts as inclusions of ilmenite. When the titanium content reaches 2–15% or more, the magnetite is termed titaniferous magnetite (Poveromo 1999). Titanium dioxide content of the present magnetite varies from 1.95 to 16.07 wt% with an average of 6.20 wt%, which can be termed as titaniferous magnetite.

The average chemical compositions of these grains compared with the other analyses of the Egyptian beach magnetite are tabulated in Table 12. The investigated magnetite is richer in SiO_2, CaO, and MnO compared with that obtained by El-Hinnawi (1964), Hammoud (1966), and El-Kammar et al. (2011). This feature may be due to the presence of silicate minerals as inclusions or alteration products (Fig. 12e). The higher total iron (e.g., Fe_2O_3) of Rosetta beach sands obtained by El-Hinnawi (1964) may be attributed to the richer magnetite concentrate in ferri-ilmenite than the others. Also, the higher contents of TiO_2 of Rosetta beach sands given by El-Kammar et al. (2011) that may be ascribed to the analyzed samples were originally titanomagnetite. Moreover, Abdel-Karim et al. (2016) revealed that the euhedral-shaped grain magnetite is lower in Fe_2O_3 than the spherical ones.

The weight percentages of the total iron oxides (e.g., Fe_2O_3) of the analyzed magnetite were graphically plotted against other oxides on scatter plot diagrams (Fig. 13a). These diagrams generally reveal the presence of negative correlation between total iron oxides and each of TiO_2, Al_2O_3,

Table 12 Comparison of studied magnetite with other Egyptian beach magnetites

Oxides	Present work	Rosetta beach (El-Hinnawi 1964)	Rosetta beach (Hammoud 1966)	Rosetta El-Kammar et al. (2011)
Fe_2O_3	85.04	92.32	79.42	74.62
TiO_2	6.20	6.20	12.35	19.94
SiO_2	3.25	0.45	1.63	0.22
Al_2O_3	2.09	0.60	2.94	1.51
CaO	0.49	tr.	0.12	0.03
MnO	0.62	tr.	0.62	0.54
Cr_2O_3	0.37	tr.	0.56	0.67
MgO	1.14	0.10	0.98	1.53
V_2O_3	0.42	0.45	0.52	0.82
Total	99.62	100.12	99.14	99.88

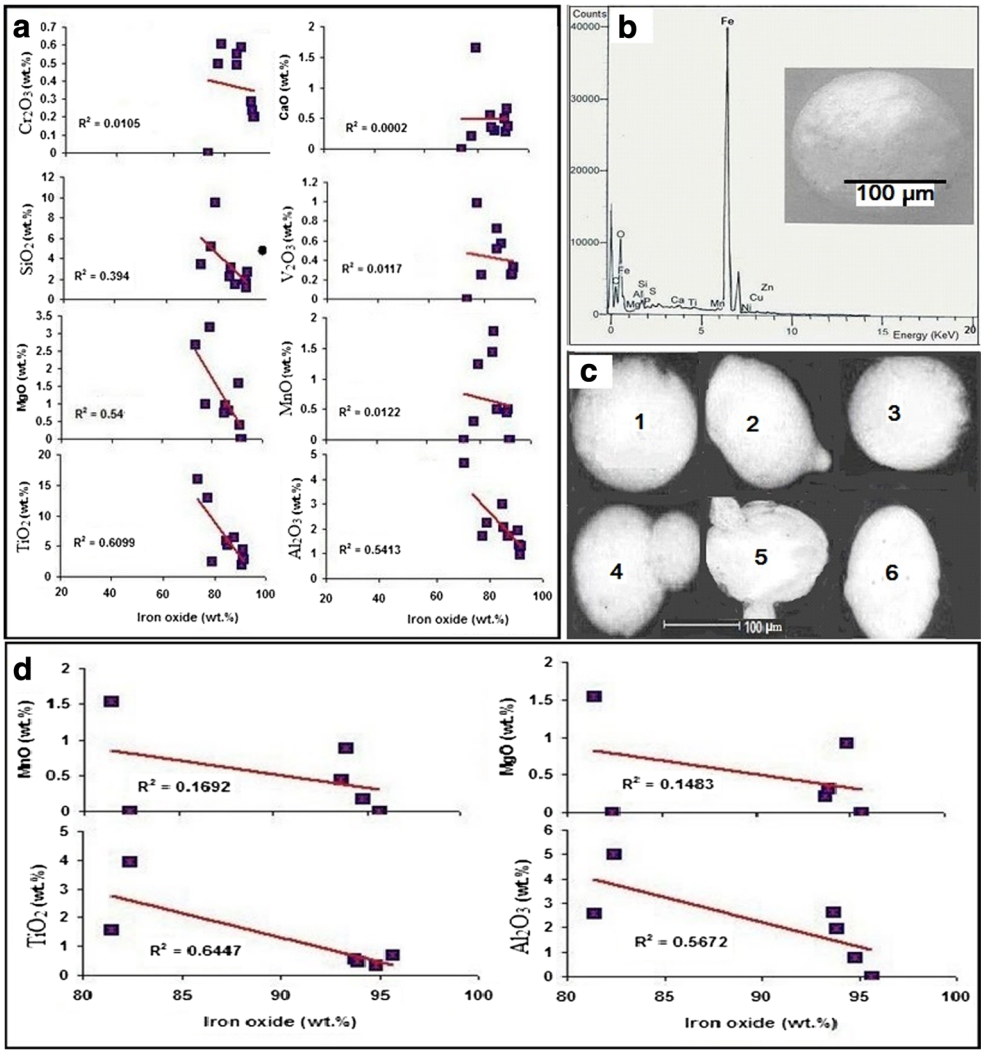

Fig. 13 **a** Scatter plot diagrams showing the relation between the total iron oxides (Fe_2O_3 total wt%) and other elements (wt%) of analyzed magnetite; **b** back-scattered electron image and ESEM chemical analysis of abnormal spherical magnetite grains; **c** back-scattered electron image of abnormal magnetite grains showing *1* spherical, *2* drop like, *3* discoid, *4* cocoon like, *5* winged, and *6* ovoid shapes; and **d** scatter plot diagrams showing the relation between total iron oxides (wt%) and TiO_2, MnO, MgO, and Al_2O_3 (wt%) of analyzed magnetite grains

CaO, MnO, SiO_2, Cr_2O_3, V_2O_3, and MgO. This feature may suggest a chemical substitution of each of these elements with Fe in the internal atomic structure of magnetite. The divalent ions may substitute Fe^{2+}, whereas the trivalent ions substitute Fe^{3+}.

Spherical magnetite grains

The abnormal grain varieties of magnetite are the most dominant. Six abnormal spherical magnetite grains were also analyzed using an environmental scanning electron microscope (Table 13). The energy-dispersive X-ray and the back-scattered electron image are represented in Fig. 13b. The abnormal magnetite grains are variable in shapes including spherical, drop like, discoid, cocoon like, winged, and ovoid shapes (Fig. 13c). The iron oxide content ranges from 81.39 to 95.63 wt% with an average of 90.29 wt%. This average is quite similar to those given by El Balaksay (2003) and Abu-Diab (2008) (92.43 and 90.99%), respectively. These data are analogues to that reported by Abdel-Karim et al. (2016), who proved that the spherical magnetite grains are higher in Fe_2O_3 than those of the euhedral-shaped grains. The average contents of MgO, Al_2O_3, and MnO are 0.50, 2.17, and 0.51%, respectively (Table 13).

The weight percentages of the total iron oxides (e.g., Fe_2O_3) were plotted against TiO_2, Al_2O_3, MnO, and MgO (Fig. 13d). Negative correlation between total iron oxides and each of TiO_2, Al_2O_3, MnO, and MgO is clearly recorded. This feature may attribute to chemical substitution of each element with Fe in the internal atomic structure of magnetite. Trace element concentrations of the analyzed grains show the presence of Cr, Ni, Nb, Ta, and V, indicating that these elements are probably hosted by magnetite (Table 13).

Implication of chemistry for magnetite genesis

The environmental SEM data indicate that magnetite concentrate are sizeable group of elements (Table 13). It contains 0.05 wt% V_2O_3, 0.18 wt% NiO, 0.99 wt% TaO, 1.69 wt%

Table 13 Chemical analysis of six spherical magnetite grains

Oxides	G.1	G.2	G.3	G.4	G.5	G.6	Av.(6)
Fe_2O_3	95.63	94.78	82.37	81.39	93.67	93.87	90.29
TiO_2	0.69	0.33	3.96	1.58	0.55	0.48	1.27
MnO	–	0.18	–	1.54	0.45	0.89	0.51
Cr_2O_3	0.73	0.34	0.79	–	–	–	0.31
V_2O_3	–	0.30	–	–	–	–	0.05
CaO	0.52	0.41	0.96	–	1.51	1.34	0.79
SO_3	1.28	–	1.38	–	–	–	0.44
SiO_2	1.15	0.29	1.39	–	–	–	0.47
Al_2O_3	–	0.76	5.04	2.58	2.66	1.99	2.17
MgO	–	0.92	–	1.55	0.22	0.32	0.50
Cl_2O	–	0.51	–	–.	–	–	0.09
P_2O_5	–	0.17	–	–	–	–	0.03
TaO	–	–	4.11	1.83	–	–	0.99
Nb_2O_5	–	1.00	–	9.12	–	–	1.69
SnO_2	–	–	–	0.37	–	–	0.06
PbO_2	–	–	–	–	0.94	–	0.16
NiO	–	–	–	–	–	1.10	0.18
Total	100.00	99.99	100.00	99.96	100.00	99.99	99.99

Nb_2O_5, 0.06 wt% SnO_2, and 0.16 wt% PbO_2 (Table 3). According to Wolfenden et al. (2005) and Garzanti et al. (2006), El-Kammar et al. (2011), and Shukri (1951), this magnetite is probably derived from the basic volcanic rocks of the Blue Nile provenance. Also, in agreement with El-Kammar et al. (1992) and Abdel-Karim et al. (2016), the high heavy metal content (V, Ni, and Pb) is indicative of the basic volcanic source. The high contents of TaO (0.99 wt%), Nb_2O_5 (1.69 wt%), and SnO_2 (0.06 wt%) are strong evidence of potential contamination by fine inclusions of other minerals such as tantalite [(Fe, Mn) Ta_2O_6], columbite [(Fe, Mn) Nb_2O_6], and cassiterite (SnO_2). Therefore, the present magnetite can be considered as a good indicator for the volcanic source of the Ethiopian plateau. Similar conclusion was recorded by El-Kammar et al. (2011) and Abdel-Karim et al. (2016).

Reserve of magnetite of the study area

The studied coastal plain area is more or less plainer surface so that the volume of sands is roughly calculated as length × width × depth in cubic meter, which attains 10 million m^3. The tonnage of the raw sand was calculated by multiplying the volume by the calculated average apparent density of the raw sand (15.9 million t). The tonnage of magnetite was calculated by multiplying the tonnage of the raw sands of the studied area by the calculated weight percentage of magnetite obtained by laboratory and ore dressing techniques, which amounts to 182,850 and 179,670 t, Table 14), respectively. This value is lower than that given by Naim et al. (1993), who concluded 1,437,000 t for reserves of placer magnetite at Rashid area, Egypt.

Conclusions

The studied north-west of El-Burullus Lake area is nearly rectangular in shape, 10 km long, covered by 306 samples to a depth of 1 m at a grid pattern 200 m × 200 m nearly parallel and perpendicular to the shoreline. The following remarks can be concluded:

1- The apparent specific gravity of field samples varies from 1.29 to 1.74 g/cm^3 with 1.59 g/cm^3 average.
2- The fine percentages range from 0.72 to 74.08 wt% with 18.00 wt% average. In winter season and during stormy condition, the coastal plain was covered by sea water rich in fines derived from clay lenses of eroded continental shelf.
3- The Bromoform heavy fractions representing economic minerals and gangue silicates vary from 34.22 to 4.78 wt% with 16.60 wt% average, whereas the Clerici's heavy fractions which represent economic heavy minerals range from 13.58 to 0.38 wt% with 3.70 wt% average.
4- The magnetite content obtained by laboratory techniques ranges from 0.11 to 2.92 wt% with 1.15 wt% average. It represents one third of the total economic minerals. Close relationships between concentration of magnetite and concentration of other economic heavy minerals were recorded. So, the magnetite content which can be easily obtained by using of a hand magnet can be considered as a pathfinder for the concentration of the associated economic minerals.
5- There are positive correlations between the average contents of magnetite and that of apparent specific gravity and total and economic heavy minerals. The magnetite content obtained by ore dressing techniques reached to 1.13 wt% with 98.26 wt% recovery.
6- The tonnage of magnetite obtained by laboratory and ore dressing techniques is 182,850 and 179,670 t, respectively.
7- Grain size of magnetite is a unimodal distribution with modal class that lies in the very fine sand size class of >93 wt% from the particles. The spherical grains are coarser than the associated magnetite concentrate. So, they are concentrated by sieving process.
8- Magnetite grains have generally irregular shape and subangular and surrounded particles. Some of them exhibit octahedron crystals; contact double twins and parting plains are also present.

Table 14 The average content (wt%) and reserve tonnage of magnetite in the studied area

Volume of study area (length × width × depth) (m^3)	Average apparent density of raw sands (t/m^3)	Tonnage of raw sands (t)		
10,000 × 1000 × 1 = 10,000,000	1.59	15,900,000		
Magnetite average content and reserve				Recovery (wt%)
Laboratory technique		Ore dressing technique		
Av. cont. (wt%)	Reserve (t)	Av. cont. (wt%)	Reserve (t)	98.26
1.15	182,850	1.13	179,670	

9- The contents of iron oxide and titanium dioxide of octahedral magnetite range from 73.29 to 91.53 and 1.95 to 16.07 wt%, with 85.04 and 6.20 wt% average, whereas those of the abnormal spherical one vary from 81.39 to 95.63 and 0.33 to 3.96 wt%, with 90.29 and 1.27 wt% average.

10- There is a negative correlation between total iron oxides and each of TiO_2, Al_2O_3, CaO, MnO, SiO_2, Cr_2O_3, V_2O_3, and MgO contents, a feature that suggests a chemical substitution of each of these elements with Fe in the magnetite internal atomic structure.

11- The chemical data obtained by ESEM suggest that the studied magnetite is probably derived from the basic volcanic rocks of the Blue Nile provenance and can be considered as a good indicator for the volcanic source of the Ethiopian plateau.

Acknowledgements The authors acknowledged the Nuclear Materials Authority, Cairo, Egypt, for their kind field and laboratory facilities during the preparation of this work.

Critical comments and constructive reviews by the three kind anonymous reviewers and the assistant editor, Prof. Mehmet Çelik, substantially improved an early version of this manuscript. Also, Editor-in-Chief Professor Abdullah Al-Amri is thanked for editorial handling.

References

Abdel-Karim AM, Zaid S, Moustafa MI, Barakat MG (2016) Mineralogy, chemistry and radioactivity of the heavy minerals in the black sands, along the northern coast of Egypt. J Afri Earth Sci 123:10–20

Abu-Diab AA (2008) Characters and distribution of the economic minerals in the black sand deposits of the coastal area, west El-Burullus, Egypt and their sedimentation condition. Dissertation, Ain Shams University

Barakat MG (2004) Sedimentological studies and evaluation of some black sands deposits on the northern coast of Egypt. Dissertation, Alexandria University

Basta EZ (1972) Different types of ilmenite-magnetite intergrowths and their origin. Bull Fac Sci, Cairo University 44:195–212

Boctor NZ (1966) Ore microscopic studies of the opaque minerals in Rosetta and Damietta black sands. Dissertation, Cairo University

Burt RO (1989) Gravity concentration technology. Elsevier Science Publishers, Amsterdam

Dabbour GA (1991) Heavy minerals content in relation to the apparent specific gravity of the Egyptian black sands. Mans Sci Bull, Special Issue :212–220

Deer WA, Howie RA, Zussman J (1975) An introduction to the rock forming minerals. Longman group Ltd., London

Dewedar AA (1997) Comparative studies on the heavy minerals in some black sands deposits from Sinai and east Rosetta with contribution to the mineralogy and economics of their garnets. Dissertation, El Menoufia University

El Balaksay SS (2003) Mineralogical studies for the economic minerals in the sand dunes belt at Baltim area, Egypt. Dissertation, Ain Shams University

El-Hinnawi EE (1964) Mineralogical and geochemical studies on Egyptian (UAR) black sands. Beitr Miner Petrogr 9:519–532

El-Kammar AA, Philip G, Arafa I (1992) Geochemistry of recent Nile sediment from the main Nile course in Egypt and the principle tributaries in Ethiopia and Sudan. Proceeding of the 1st International conference on the Geology of the Arab Word, Cairo Univ, pp 527–541

El-Kammar AA, Ragab AA, Moustafa MI (2011) Geochemistry of economic heavy minerals from Rosetta black sand of Egypt. JKAU, Earth Sci 22:2–17

El-Nahas HA (2002) Mineralogy, evaluation and upgrading studies on some economic minerals in beach black sands, El Arish area, Egypt. Dissertation, El Menoufia University

Garzanti E, Ando S, Vezoli G, Abdel Megid AA, El-Kammar A (2006) Petrology of Nile River sands (Ethiopia and Sudan): sediment budgets and erosion patterns. Earth and Planet Sci Let 252:327–341

Hammoud NMS (1966) Concentrations of monazite from Egyptian black sands employing industrial techniques. Dissertation, Cairo University

Kelly EG, Spottiswood DJ (1989) The theory of electrostatic separations: a review, part I. Fundamentals. Minerals Eng 2:3–46

Lawver JE, Taylor JB, Knoll FS (1986) Laboratory testing for electrostatic concentration circuit design. SME-AIME Annual Meeting, March, pp 454–477

Moustafa MI (1999) Mineralogy and beneficiation of economic minerals in the Egyptian black sands. Dissertation, El Mansoura University

Moustafa MI (2007) Separation flow sheet for high purity concentrates of some Ec. Min. from El-Burullus Baltim sand Dunes Area, North coast, Egypt. The fifth international conference on the geology of Africa 1:111–124

Naim G, El-Melegy ET, El Azab A (1993) Black sand assessment. The Egyptian Geological Survey, p 67

Nofal AM, El Tawil SZ, Aly FH (1980) Mise en valuer de la magnetite titanifere de gisements de sable cotier due Delta d'Egypte. Industrie Mineral les Techniques 80:203

Poveromo JJ (1999) Iron ores. Technology—international, Quebec Cartier Mining Company. AISE Steel Foundation, Pittsburgh, PA. Chapter 8, pp 457–642

Shukri NM (1951) Mineral analysis tables of some Nile sediments. Bull Inst Desert d'Egypt 1(1):39–67

Wassef SN, Mikhail MA (1981) Distribution and mineralogy of ilmenite and other accessory minerals in the beach sands of west Rosetta, Egypt. Desert Instit Bull, ARE 31:17–29

Wolfenden E, Ebinger C, Yirgu G, Renne P, Kelley SP (2005) Evolution of a volcanic rifted margin, Southern Red Sea, Ethiopia. Bull Geol Soc Am 117:846–864